^{13}C NMR and relaxation studies of the nanomagnet Mn$_{12}$-acetate

Randall M. Achey

Department of Chemistry, Florida State University, Tallahassee, Florida 32306
and National High Magnetic Field Laboratory, Tallahassee, Florida 32310

Philip L. Kuhns and Arneil P. Reyes

National High Magnetic Field Laboratory, Tallahassee, Florida 32310

William G. Moulton

Department of Physics, Florida State University, Tallahassee, Florida 32306
and National High Magnetic Field Laboratory, Tallahassee, Florida 32310

Naresh S. Dalal*

Department of Chemistry, Florida State University, Tallahassee, Florida 32306
and National High Magnetic Field Laboratory, Tallahassee, Florida 32310

The nanomagnet $[Mn_{12}O_{12}(CH_3COO)_{16}(H_2O)_4]\cdot 2CH_3COOH\cdot 4H_2O$, also known as Mn$_{12}$, has been synthesized with ^{13}C labeling at the CH$_3$ groups, and investigated by ^{13}C NMR at fields up to 23 T. Using oriented samples, it is possible to resolve four distinct ^{13}C peaks at room temperature, located on both sides of the unshifted Larmor frequency. These peaks were assigned to the four hyperfine-shifted, magnetically inequivalent sets of ^{13}CH$_3$ groups in the Mn$_{12}$ lattice, based on a comparison with the crystal structure and point-dipole and spin-density calculations. These results establish that the unpaired electron spin density of the $S=10$ system in this cluster extends over the entire molecular framework, not just the core. These results are discussed in relationship to inelastic neutron scattering measurements. The temperature and field dependence of the ^{13}C nuclear-spin-lattice-relaxation time T_1 on the least shifted peak was measured. A single weakly field-dependent minimum at about 60 K is observed in the temperature dependence of the measured T_1. The relaxation mechanism responsible for the T_1 minimum is ascribed mainly to hindered rotation of the methyl group of the acetate ligand at higher temperature, and to electronic spin fluctuations at lower temperature.

I. INTRODUCTION

This paper reports on our ^{13}C NMR measurements on oriented samples of the molecular nanomagnet $[Mn_{12}O_{12}(CH_3COO)_{16}(H_2O)_4]2CH_3COOH4H_2O$, hereafter Mn$_{12}$, which was first synthesized by Lis.[1] The primary reason for the focus on this compound is that it was the first example of an assembly of well-oriented, isolated molecules that behave like nanomagnets, with well-defined quantum jumps in their magnetization hysteresis loops[2] below 3 K. The core of Mn$_{12}$ consists of two subsystems of Mn ions with mixed valences. The outer subsystem comprises a crown of eight Mn^{+3} ($S=2$) ions, coupled ferromagnetically with a total spin of $S_1=16$, while the inner system is a tetrahedron of Mn^{+4} ($S=3/2$) ions, also coupled ferromagnetically with a total spin of $S_2=6$. The two subsystems couple antiferromagnetically, to yield an overall spin of $S_1-S_2=10$. The Mn$_{12}$ cluster thus behaves as an entity with a ground state of $S=10$, exhibiting many interesting properties, and has been the subject of extensive theoretical[3–12] and experimental[13–27] work. The present investigation was motivated by several factors. First, earlier NMR studies, utilizing ^1H, ^2H, and μSR spin-lattice relaxation time (T_1) measurements,[15,27,28] indicated the presence of spin dynamics possibly related to QTM, but the interpretations were rather different. The ^1H and μSR T_1 relaxation mechanisms were interpreted as being due to thermal fluctuations be-

tween the possible $2S+1$ (i.e., 21) spin levels, without an interpretation of the T_1 minimum around 60 K, while the ^2H data indicated the presence of both molecular motion and spin fluctuation effects. Another important issue was that both the ^1H and ^2H NMR studies detected a stretched exponential recovery curve, i.e., with magnetization recovery of the form

$$M(t) = M_0(1 - e^{-(t/T_1)^\alpha}), \qquad (1.1)$$

where M_0 is the equilibrium magnetization and α is the stretched exponent, in relaxation measurements at all temperatures. This was interpreted in both cases as being a result of many different environments being present in the lattice.[27,28] On the other hand, this stretched exponential behavior is also known to be a characteristic of spin-glass behavior in magnetic systems.[29] Thus the exact mechanism of this phenomenon was not clear. Additionally, the ^2H data showed two minima in T_1,[27] while only one minimum was observed in this study and the ^1H study.

One of the difficulties in previous studies was that the samples used were unoriented powders, which led to broad, poorly resolved NMR peaks. As a consequence, the observed relaxation data were potentially a superposition of that from all the 72 different proton or deuteron sites with a distribution of orientations. In the present work we have attempted to clarify these issues by (a) making measurements on oriented samples; (b) utilizing the ^{13}C nucleus as a probe, which is one bond closer to the Mn ions than protons or
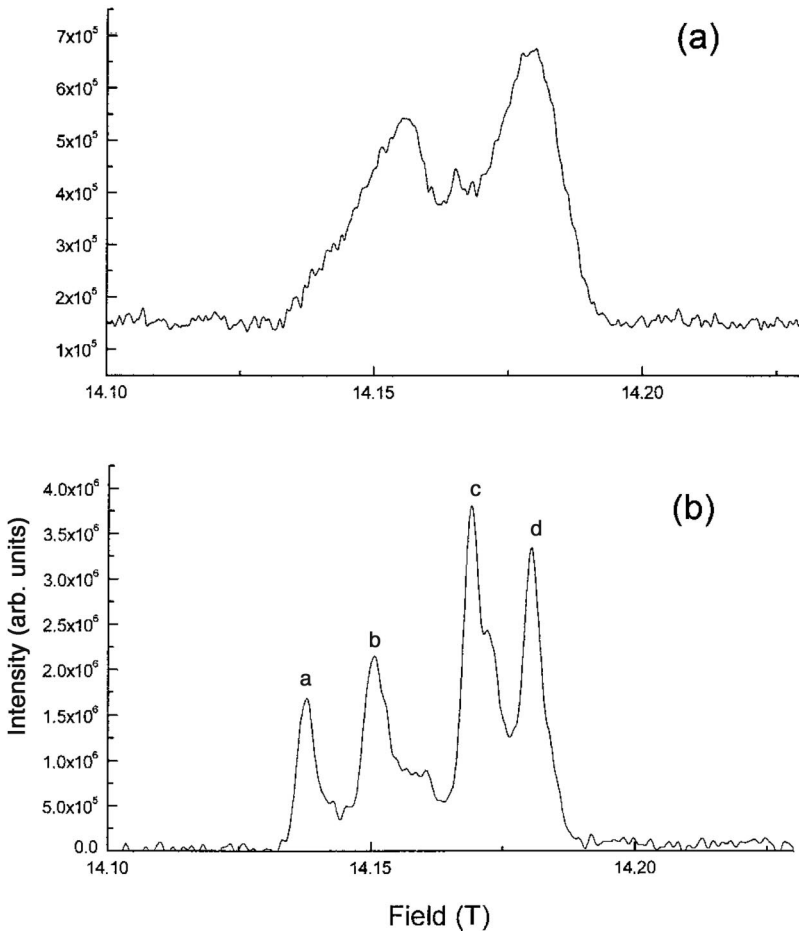
FIG. 1. Comparison of the ^{13}C NMR spectra at 250 K and 151.7 MHz of 2-^{13}C Mn$_{12}$: (a) an unoriented powder, and (b) an oriented sample with H parallel to the c axis. Note the much higher resolution obtained with the oriented sample.

deuterons, and would thus be expected to be more sensitive to the Mn spin fluctuations; and (c) utilizing Zeeman fields up to 23 T, and temperatures down to 1.8 K in order to probe more thoroughly the nature of the spin fluctuations in the Mn$_{12}$ lattice. We have successfully synthesized ^{13}C-labeled Mn$_{12}$, and believe that the presently reported ^{13}C results complement the earlier reported ^1H and ^2H data. We will attempt to demonstrate that ^{13}C NMR is a sensitive probe of the spin fluctuations in the Mn$_{12}$-type nanomagnetic lattices. To our knowledge, this is the first ^{13}C NMR study on any compound in this class of materials with large electronic spin in the ground state.

II. EXPERIMENTAL DETAILS

Samples were prepared with ^{13}C labeling at the CH$_3$ sites. This labeling was accomplished by carrying out the synthesis as reported by Lis,[1] but substituting acetic acid that was labeled at the methyl carbon position, $^{13}CH_3COOH$, henceforth 2-^{13}C. The $^{13}CH_3COOH$ was purchased from Aldrich and used as received. It was not possible to grow single crystals large enough for the NMR studies. The crystallites obtained were about 0.1-mm-long needles, with an aspect ratio of about 10, and with the long axis as the crystallographic c axis in the tetragonal ($1\bar{4}2d$) system. The sample authenticity was verified by dc as well as ac magnetization measurements, which showed the characteristic frequency-dependent maxima as reported in earlier work.[30] The dc magnetic susceptibility was measured with a Quantum Design superconducting quantum interference device (SQUID) magnetometer, while a Quantum Design PPMS was utilized for measuring the ac susceptibility. Oriented samples were prepared by mixing the polycrystalline powder, which was sieved with a 120 mesh, with Stycast 1266 epoxy, and allowing it to set at room temperature in a 7-T magnetic field. The sample alignment was confirmed by noting the anisotropy of the ^{13}C NMR spectrum. Additionally, the ^{13}C NMR spectrum of an unoriented 2-^{13}C-enriched powder sample exhibited two broad lines at room temperature, as compared to a well-resolved quartet for the oriented sample, as shown in Fig. 1.

NMR measurements were performed with the alignment axis parallel as well as perpendicular to the Zeeman field up to 23 T, and at temperatures of 1.8–296 K. A water-cooled resistive magnet was used for the 23-T measurements, while a superconducting magnet was used for all others. A Tecmag Aries/Libra spectrometer was used, with a home-built NMR probe. Due to the large width of the spectrum, ranging from 400 kHz at 296 K to 3 MHz at 1.8 K, data were acquired by stepping the magnetic field. Hahn echo pulse sequences were used for these acquisitions. These spectra were then Fourier-transformed, scaled, and summed using the technique reported earlier.[31] Spin-lattice-relaxation time (T_1) measurements were performed on the highest-field-shifted peak in
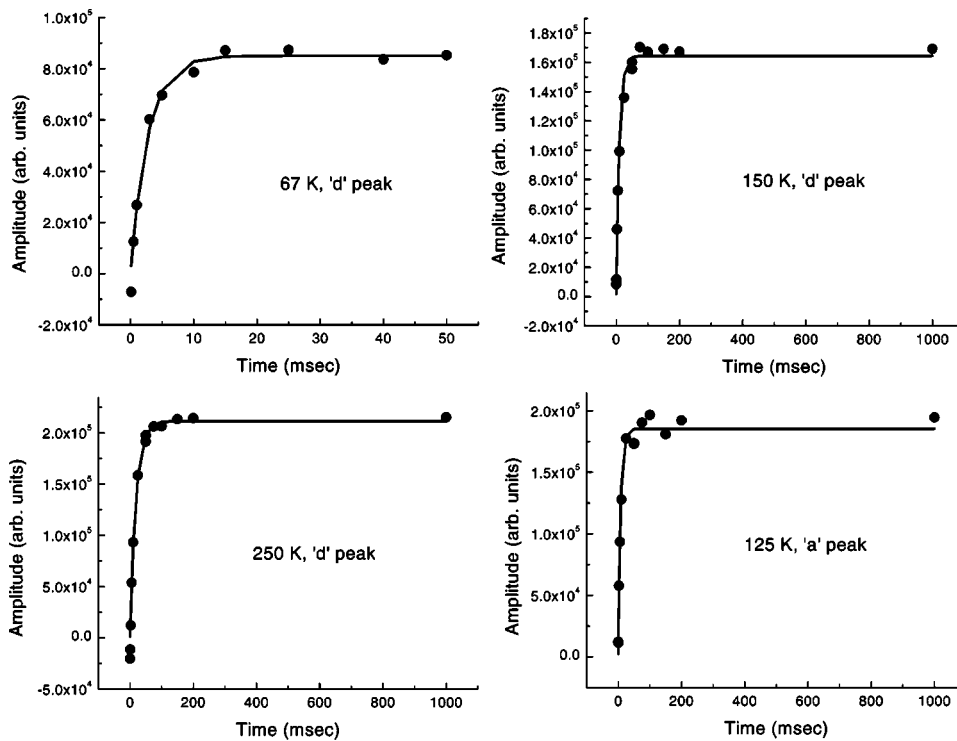
FIG. 2. Examples of single exponential fits to the nuclear magnetization recovery of the aligned 2-[13]C Mn$_{12}$ sample as measured on (a) the d peak at 67 K, (b) the d peak at 150 K, (c) the d peak at 250 K, and (d) the a peak at 125 K.

the ^{13}C NMR spectrum (peak d in Fig. 1, *vide infra*). This decision was arrived at because the d peak remained visible to the lowest temperature of any of the shifted peaks. Nuclear magnetization recovery curves were acquired by a saturation recovery pulse sequence with Hahn echo inspection. The recovery curves showed single exponential behavior of the form

$$M(t) = M_0\{1 - \exp[-(t/T_1)]\} \qquad (2.1)$$

from 296 down to 10 K, in contrast to the ^{1}H and ^{2}H measurements where the recovery showed stretched exponential behavior at all temperatures. Below 10 K the lines overlap, and the recovery showed stretched exponential behavior. No proton decoupling was employed, since the main source of peak broadening was of electronic origin.

III. EXPERIMENTAL RESULTS AND INTERPRETATION

Figure 1 shows two examples of ^{13}C spectra obtained (a) from a powder and (b) from the oriented Mn$_{12}$ sample, with H parallel to the c axis. The better resolution afforded by the oriented sample is evident here. The magnetization recovery was found to be single exponential, examples of which is shown in Fig. 2. Figure 3 compares spectra taken at 57.5, 151.7, and 223 MHz. An additional splitting of the highest-field d peak is evident at 223 MHz, which is not yet understood.

A. Peak assignment

Figure 1(b) depicts the ^{13}C NMR spectrum of the aligned sample at 296 K and 151.7 MHz for H parallel to the c axis. The observed signal was generally a quartet, as can be noted from the figure. The peaks have been labeled a, b, c, and

d, from lowest field to highest field. The peaks were assigned based on the known crystal structure,[1] and the fact that only the CH$_3$ were labeled. A schematic of the structure of the molecule is shown in Fig. 4, with emphasis placed on the methyl carbons. The peak assignment is as follows: (i) The lowest field peak, labeled a, is assigned to the methyl carbons on the acetate ligands bridging between the outer ring Mn ions and oriented axially [marked a in Fig. 4]. The magnetic moments of the outer ring Mn ions are oriented parallel to the magnetic field in the ground state, and would contribute a magnetic field to these carbon nuclei that is parallel to the applied field, causing a shift of resonance to a lower field. (ii) The b peak is assigned to the carbons of the methyl groups on the acetates bridging between the outer ring Mn ions and positioned close to the inner Mn ions. The dipolar field contributions of these will tend to cancel, providing a shift that is smaller than the a carbons, moving the b peak closer to the unshifted center position. (iii) The unshifted c peak can be attributed to the CH$_3$ groups of the acetic acid molecules solvated in the crystal lattice, which are expected to interact only weakly with the cluster, and to a minor contribution from the natural abundance ^{13}C nuclei in the epoxy used to align the sample (as checked by measurements on a blank epoxy sample). The methyl carbon nuclei not covalently bonded to the molecules are farthest from the Mn electronic moments, and therefore would be least affected by them. (iv) The highest-field d peak is assigned to four of the methyl carbons on the radially oriented acetate ligands and the four methyl carbons on acetate ligands bridging between inner and outer Mn ions [marked as d in Fig. 4]. The latter methyl carbons have magnetic-field contributions with the inner Mn ions dominating, leading to a shift to resonance at higher field. For the positions on the perimeter of the cluster, the contribution to the dipolar field is mainly from the Mn
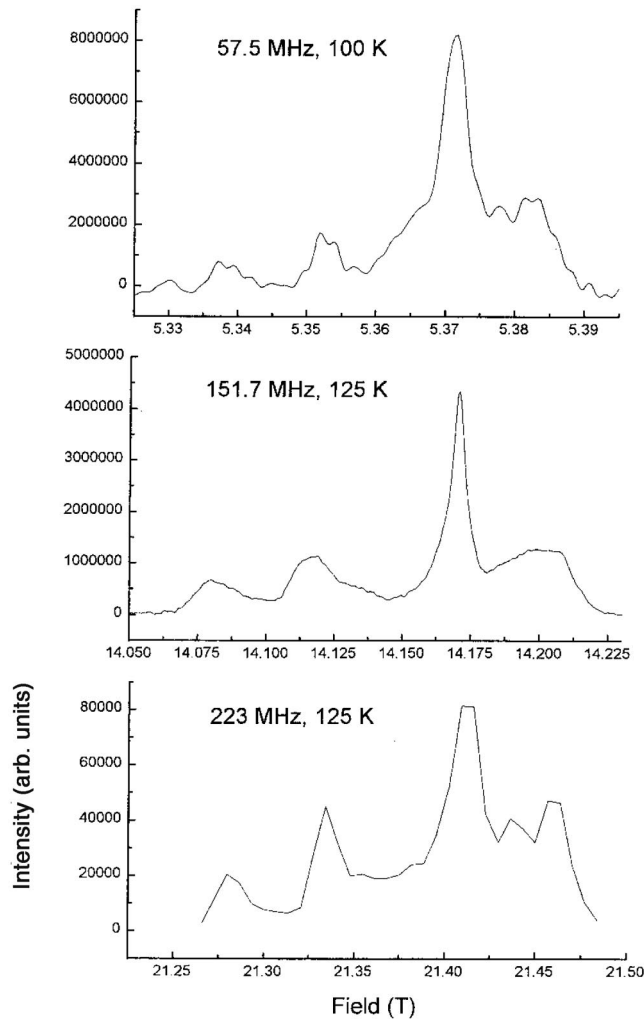
FIG. 3. Comparison of the ^{13}C spectrum at 57.5, 151.7 MHz, and 223 MHz.

ions on the outer crown of eight. The dipolar field at the perimeter positions due to these Mn ions will be opposed to the applied magnetic field, because the magnetic moments of the outer Mn ions align with the magnetic field in the ground state, and these carbon nuclei are positioned on a line perpendicular to the moments. This also leads to a shift to a higher resonance field.
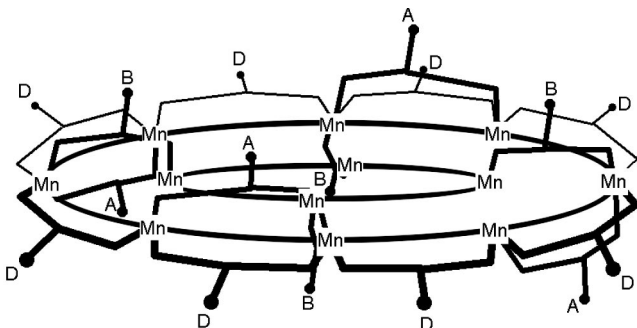
FIG. 4. A schematic of the structure of the molecule with methyl carbon sites labeled according to their peak assignment.

Additional support for these assignments was provided by an approximate calculation of the dipolar fields at the various ^{13}C sites. This was accomplished by employing a point-dipole model, using the atomic positions as reported by Lis.[1] In this model, the dipole field at a single ^{13}C site is a sum of the contributions of the fields from all of the individual Mn ions, given by

$$v(j) = \sum_i \frac{3(\mu_i \times r_{ij} - \mu_i |r_{ij}|^2)}{r_{ij}^5}, \quad (3.1)$$

where μ_i is the point moment of each Mn ion, and r_{ij} is the vector from each Mn ion to the ^{13}C atom. A comparison of these results with the experimental findings is listed in Table I. The experimental shifts agree in direction with the calculations, but only in the trend as regards magnitude, as may be expected from a point-dipole calculation (i.e., the point-dipole model will only qualitatively describe the system). This simulation, nevertheless, supports our peak assignments. An additional splitting of the d peak is predicted by the point-dipole calculations. In fact, a splitting of the d peak was observed at a higher field: 223 MHz. These two lines may overlap and be indistinguishable at 151.7 MHz, but separate at a higher field.

Further study has been carried out on the dependence of the ^{13}C spectrum on the orientation of the c axis of the aligned sample with respect to the applied magnetic field. This has shown that there are both isotropic and anisotropic contributions to the local magnetic field at the ^{13}C sites. The anisotropic contribution follows a $(3 \cos^2\theta - 1)$ dependence, which indicates that this is a dipolar field. The presence of an isotropic contribution to the magnetic field at the ^{13}C sites shows that there is electron-spin delocalization present at these sites. The unpaired electron-spin density at the three shifted sites has been deduced from these measurements. The fields present at the three different shifted sites are 140, 65.4, and -32.7 G, respectively for the a, b, and d peaks. This corresponds to 0.105, 0.0488, and -0.0244 fraction of an electron on the sites, respectively. This is based on the fact that a single electron present at a ^{13}C nucleus gives a shift of 1340 G.[32]

The above-discussed detection of unpaired electron spin density on the ^{13}C sites complements a recent inelastic neutron scattering (INS) study.[33] In the INS measurements, there was no spin density found on the oxygen atoms; however, the spin density on the manganese atoms was less than predicted. The spin density found on the carbon atoms in this study may account for this deficiency.

B. Temperature dependence of the ^{13}C spectrum

Since a major goal was to probe the spin fluctuation dynamics, we undertook detailed studies of the temperature dependence of the peak positions, linewidth, and spin-lattice relaxation time T_1. Figure 5 shows the shift of the ^{13}C NMR lines from the unshifted resonance field as a function of temperature for an observation frequency of 151.7 MHz. The shifts increase with lowering temperature. The dc susceptibility follows a Curie-Weiss behavior, which leads to increased magnetic broadening at lower temperature. The a

TABLE I. Comparison of measured dipole fields and calculated dipole fields.

Methyl carbon set	Experimental shift at 296 K (Oe)	Calculated shift (Oe/μ_B)
a	261.3	448.1
b	146.4	68.2
c	0.7	-82.6
$d1$	-38.4	-120.6
$d2$	-38.4	-144.9

and b peaks thus become unobservable below about 100 K due to excessive line broadening and consequently a low signal-to-noise ratio. The d peak, being less shifted and less broadened than the a and b peaks, can be followed down to the lowest temperature measured. Figure 6 shows the shift of the peaks versus the measured overall dc magnetic susceptibility, χ. The χ data used were obtained on a SQUID magnetometer as a function of temperature at a fixed field of 100 Oe on a single crystal of Mn_{12}, with H parallel to the c axis. The shift of the NMR peaks tracks linearly with χ at higher temperatures, above 100 K. If this trend is extrapolated to lower χ, or higher temperature, these shifts converge to zero at a susceptibility value corresponding to a temperature of about 1000 K. Above this temperature, it appears that all coupling between the Mn ions within each cluster has been overcome by thermal agitation. It should be noted that this temperature value is much higher than the estimated exchange energies in the Mn_{12} cluster, which are less than 200 K.[34] The only remaining magnetic susceptibility is the temperature-independent part, χ_0. At lower temperature, below about 100 K, the relationship between the NMR peak shift and χ begins to deviate from linearity, with the shift becoming less dependent on χ. This implies that the coupling between the carbon nuclei and the Mn electrons decreases as the temperature is lowered below 100 K. Conceivably, this could be caused by some type of subtle structural distortion at the Mn sites. Additional information on the
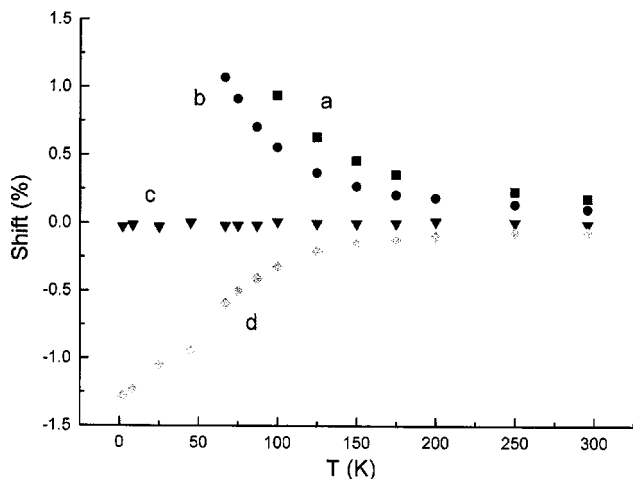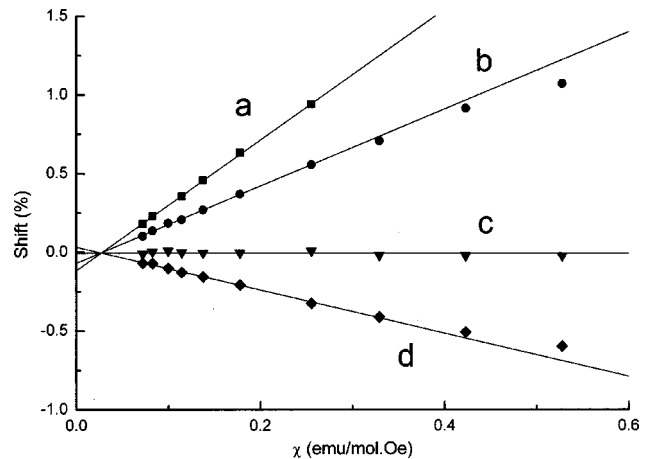
FIG. 6. Plot of the shift of the lines in the ¹³C NMR spectrum of the oriented sample as a function of the measured dc magnetic susceptibility.

magnetic coupling between the electronic and the nuclear spins was obtained from T_1 measurements, as summarized in Sec. III C.

C. Temperature and field dependence of the spin-lattice- relaxation time, T_1

Figure 7 shows the spin-lattice-relaxation rate, T_1, as a function of temperature, as measured on the d peak at a frequency of 151.7 MHz. A minimum in T_1 is observed around 60 K. Magnetization recovery was observed as a single exponential at temperatures above 10 K. As mentioned above, Fig. 2 shows examples of relaxation curves for different temperatures and also for different peaks. The curves were fit to Eq. (1). Attempts to fit these to a stretched exponential,

$$M(t) = M_0\{1 - e[(-t/T_1)^\alpha]\}, \qquad (3.2)$$

where α is the stretched exponent, yields $\alpha = 1$. This can be contrasted with the earlier data on ^1H and ^2H nuclei where stretched exponential recovery was observed[15,27] at all tem-

FIG. 5. Plot of the shift of the lines in the ¹³C NMR spectrum of the oriented sample as a function of temperature.
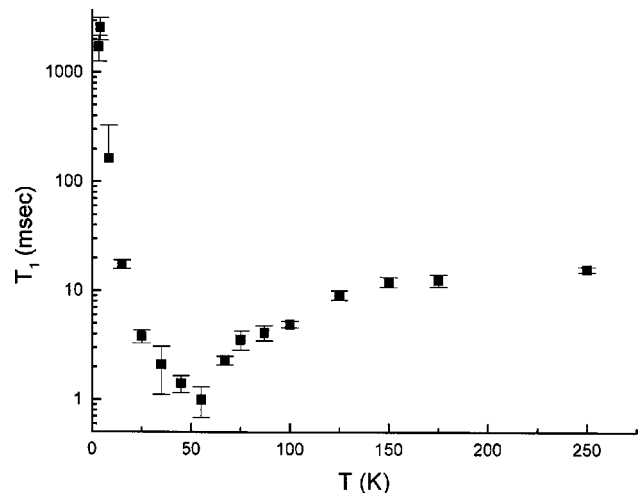
FIG. 7. Plot of the spin-lattice-relaxation time T_1, as measured on the d peak, as a function of temperature.
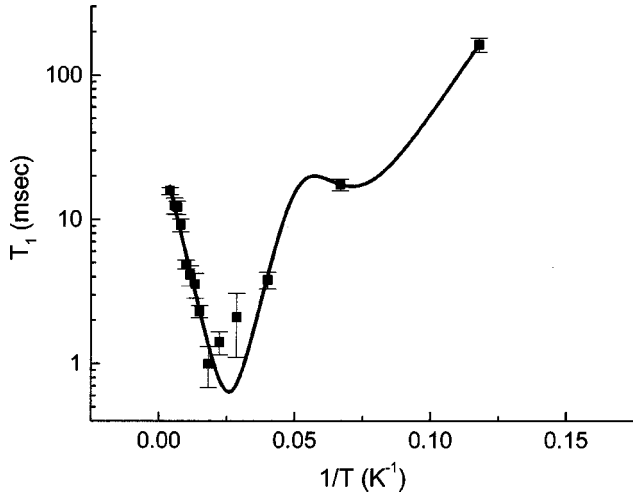
FIG. 8. Semilog plot of T_1 as a function of $1/T$, overlaid with a fit to the BPP model (continuous line).

peratures. In those studies, relaxation measurements were performed on the unshifted peak in the spectrum, to which signals from a distribution of many nuclear sites contribute.

A plot of T_1 vs temperature T, with a minimum at a certain T, generally indicates that the correlation time for some local fluctuation falls in the range of the Larmor frequency ω_L. A simple model that may be applied here is the classic Bloembergen, Purcell, and Pound (BPP) model,[35] where T_1 is given by the relation

$$\frac{1}{T_1} = \frac{\tau}{1 + \omega_L^2 \tau^2}, \tag{3.3}$$

where τ is the characteristic correlation time for the relaxation mode, and ω_L is the Larmor frequency. At points lower in temperature than the minimum, i.e., the "slow motion" regime, $\omega_L^2 \tau^2 \gg 1$, and the log of the relaxation time is linear in T. Similarly, at points higher in temperature than the minimum, in the so-called "fast motion" regime, $\omega_L^2 \tau^2 \ll 1$, and the log of T_1 is again linear in T. Figure 8 shows a plot of the measured T_1 as a function of inverse temperature. The linearity on either side of the minimum in T_1 indicates Arrhenius-type activation, and invites a fit to the BPP model. However, the slopes are different on the two sides of the minimum, suggesting that there are at least two different relaxation mechanisms. An attempt was made to fit the data to a BPP model with two different modes of relaxation. The solid line in Fig. 8 is a fit to the model. The fitting equation is

$$\frac{1}{T_1} = A \frac{\tau_1}{1 + \omega_L^2 \tau_1^2} + B \frac{\tau_2}{1 + \omega_L^2 \tau_2^2}, \tag{3.4}$$

where τ_1 and τ_2 are the correlation times for the two relaxation modes, ω_L is the Larmor frequency, and A and B are weighting coefficients for each mode. The correlation times were fit with Arrhenius-type activation according to

$$\tau_i = \tau_{i0} e^{\left(\frac{E_{ai}}{k_B T}\right)}, \tag{3.5}$$

where τ_{i0} is the inverse of the attempt frequency for the relaxation mode, e is the base of the natural logarithm, E_{ai} is the activation energy for the relaxation mode, k_B is Boltzmann's constant, and T is the absolute temperature. The fitted activation energy E_a/k_B on the high-temperature side of the minimum is 183 K, while on the low-temperature side it is 64 K. At temperatures above the minimum in T_1, the main relaxation mechanism appears to be hindered methyl group rotation. The activation energy for the mode, 183 K or 1.53 kJ/mol, compares to that for a low-hindered methyl rotor.[36-40] Relaxation due to electronic spin fluctuations dominates on the low-temperature side, with an activation energy, of 64 K, in excellent agreement with the value for the barrier for electronic spin reorientation, 64 K, as measured by ac susceptibility.[17] This agreement of the value of the relaxation barrier on the low-temperature side of the minimum with the value of the anisotropy barrier may just be fortuitous. But this agrees with the ^2H work in that the relaxation mechanism in this temperature range was attributed to electronic spin fluctuations.

Comparison of the ^{13}C T_1 data with that for ^1H and ^2H establishes the following: (i) The temperature corresponding to the T_1 minimum, about 60 K, is largely independent of frequency. This is evident from the ^{13}C data at 151.7 and 57.5 MHz, and from the ^1H data[15] at 87 and 200 MHz. (ii) The magnitude of T_1 is generally independent of frequency, especially at temperatures above the minimum. (iii) At a given temperature, the measured T_1 for ^{13}C is shorter than that for ^2H, and longer than that for ^1H. One would generally expect the relaxation for ^{13}C to be faster than that for ^1H within a methyl group, but this may be explained by the fact that the ^1H T_1 values were estimated[15] from the initial, fastest part of the recovery curves. This comparison is also complicated by the fact that both the ^1H and ^2H measurements were taken on the peak that was unshifted with respect to the position of the corresponding diamagnetic peaks, and as mentioned earlier contains signal from a variety of sites.

IV. CONCLUSIONS

From this work we have concluded the following: (i) The paramagnetic spin density of the Mn_{12} cluster is delocalized over the entire molecule, since the NMR peaks of all the methyl-carbon sites in the molecule are strongly shifted from their normal positions in the CH_3COO^- ligands in diamagnetic compounds. In addition, a significant part of this shift is isotropic in nature, while the remaining portion of the shift shows orientation dependence in accordance with a dipolar field. This result is important in that there is no long-range ordering in this compound down to the lowest measured temperature, 20 mK. The lack of ordering is thus not due to the lack of delocalization of the spin density. Other theoretical explanations for this phenomenon are required. (ii) The paramagnetic shifts are strongly temperature dependent. The temperature dependence scales with χ at temperatures above 100 K, with all the plots converging to zero shift at a χ value of 0.028 emu/mol, as extrapolated from a Curie-Weiss fit. This value of the susceptibility would correspond to a temperature of about 1000 K. At this temperature and above, the suscep-

tibility is just the temperature-independent paramagnetic susceptibility, χ_0, and all couplings between the Mn ions are broken. The measured shifts are in only qualitative agreement with those calculated by a simple point-dipole model. (iii) The measured T_1 exhibits a well-defined minimum at about 60 K, at both 57.5 and 151.7 MHz. The temperature of the minimum in T_1 is in agreement with the earlier reported T_1 data for deuterons and for protons, except for deuterons a second minimum was seen at 10 K. (iv) The nuclear magnetization recovery curves were found to be well-described by a single exponential model at temperatures above 10 K. This is in contrast to the earlier data on ^1H and ^2H. The difference is ascribed to focusing on a single type of ^{13}C site and using an oriented sample. Thus the Mn_{12} lattice does not behave like a spin-glass system.

---

*Email address: dalal@chemmail.chem.fsu.edu.

[1] T. Lis, Acta Crystallogr. **36**, 2042 (1980).

[2] J.R. Friedman, M.P. Sarachik, J. Tejada, and R. Ziolo, Phys. Rev. Lett. **76**, 3830 (1996); L. Thomas, F. Lionti, R. Ballou, D. Gatteschi, R. Sessoli, and B. Barbara, Nature (London) **383**, 145 (1996).

[3] E.M. Chudnovsky and J. Tejada, *Macroscopic Quantum Tunneling of the Magnetic Moment* (Cambridge University Press, Cambridge, 1998).

[4] *Quantum Tunneling of the Magnetization – QTM '94*, Vol. 301 of *NATO Advanced Study Institute, Series E Applied Sciences*, edited by L. Gunther and B. Barbara (Kluwer, Dordrecht, 1995).

[5] J. Villain, F. Hartman-Boutron, R. Sessoli, and A. Rettori, Europhys. Lett. **27**, 159 (1994).

[6] P. Politi, A. Rettori, F. Hartmann-Boutron, and J. Villain, Phys. Rev. Lett. **75**, 537 (1995).

[7] E.M. Chudnovsky and D.A. Garanin, Phys. Rev. Lett. **79**, 4469 (1997).

[8] H. de Raedt, S. Miyashita, K. Saito, D. Garcia-Pablos, and N. Garcia, Phys. Rev. B **56**, 11 761 (1997).

[9] D.A. Garanin and E.M. Chudnovsky, Phys. Rev. B **56**, 11 102 (1997).

[10] M.R. Pederson and S.N. Khanna, Phys. Rev. B **59**, R693 (1999).

[11] A. Fort, A. Rettori, J. Villain, D. Gatteschi, and R. Sessoli, Phys. Rev. Lett. **80**, 612 (1998).

[12] N.V. Prokof'ev and P.C.E. Stamp, Phys. Rev. Lett. **80**, 5794 (1998).

[13] J.A.A.J. Perenboom, J.S. Brooks, S. Hill, T. Hathaway, and N.S. Dalal, Phys. Rev. B **58**, 330 (1998).

[14] S. Hill, J.A.A.J. Perenboom, N.S. Dalal, T. Hathaway, T. Stalcup, and J.S. Brooks, Phys. Rev. Lett. **80**, 2453 (1998).

[15] A. Lascialfari, D. Gatteschi, F. Borsa, A. Shastri, Z.H. Jang, and P. Carretta, Phys. Rev. B **57**, 514 (1998).

[16] J. Dolinsek, D. Arcon, R. Blinc, P. Vonlanthen, J.L. Gavilano, H.R. Ott, R.M. Achey, and N.S. Dalal, Europhys. Lett. **42**, 691 (1998).

[17] A.M. Gomes, M.A. Novak, R. Sessoli, A. Caneschi, and D. Gatteschi, Phys. Rev. B **57**, 5021 (1998).

[18] P.C.E. Stamp, Nature (London) **383**, 125 (1996).

[19] R. Blinc, P. Cevc, D. Arcon, N.S. Dalal, and R.M. Achey, Phys. Rev. B **63**, 212401 (2001).

[20] M. Hennion, L. Pardi, I. Mirebeau, E. Suard, R. Sessoli, and A. Caneschi, Phys. Rev. B **56**, 8819 (1997).

[21] J.F. Fernandez, F. Luis, and J. Bartolome, Phys. Rev. Lett. **80**, 5659 (1998).

[22] F. Fominaya, J. Villain, P. Gandit, J. Chaussy, and A. Caneschi, Phys. Rev. Lett. **79**, 1126 (1997).

[23] A.A. Mukhin, V.D. Travkin, A.K. Zvezdin, S.P. Lebedev, A. Caneschi, and D. Gatteschi, Europhys. Lett. **44**, 778 (1998).

[24] A.L. Barra, D. Gatteschi, and R. Sessoli, Phys. Rev. B **56**, 8192 (1997)).

[25] J.M. Hernandez, X.X. Zhang, F. Luis, J. Tejada, J.R. Friedman, M.P. Sarachik, and R. Ziolo, Phys. Rev. B **55**, 5858 (1997).

[26] F. Luis, J. Bartolome, J.F. Fernandez, J. Tejada, J.M. Hernandez, X.X. Zhang, and R. Ziolo, Phys. Rev. B **55**, 11 448 (1997).

[27] D. Arcon, J. Dolinsek, T. Apih, R. Blinc, N.S. Dalal, and R.M. Achey, Phys. Rev. B **58**, R2941 (1998).

[28] A. Lascialfari, Z.H. Jang, F. Borsa, P. Carretta, and D. Gatteschi, Phys. Rev. Lett. **81**, 3773 (1998).

[29] R.V. Chamberlin, G. Mozurkewich, and R. Orbach, Phys. Rev. Lett. **52**, 867 (1984).

[30] A. Caneschi, D. Gatteschi, and R. Sessoli, J. Am. Chem. Soc. **113**, 5873 (1991).

[31] W.G. Clark, M.E. Hanson, F. Lefloch, and P. Segransan, Rev. Sci. Instrum. **66**, 2453 (1995).

[32] *NMR of Paramagnetic Molecules*, edited by G.N. LaMar, W. DeW. Horrocks, Jr., and R.H. Holm (Academic Press, New York, 1973).

[33] R.A. Robinson, P.J. Brown, D.N. Argyriou, D.N. Hendrickson, and S.M.J. Aubin, J. Phys.: Condens. Matter **12**, 2805 (2000).

[34] M.I. Katsnelson, V.V. Dobrovitski, and B.N. Harmon, Phys. Rev. B **59**, 6919 (1999).

[35] N. Bloembergen, E.M. Purcell, and R.V. Pound, Phys. Rev. **73**, 679 (1948).

[36] A. Buekenhoudt and L. van Gerven, Phys. Rev. B **46**, 5377 (1992).

[37] W. Muller-Warmuth, R. Schuler, M. Prager, and A. Kollmar, J. Magn. Reson. **34**, 83 (1979).

[38] D.G. Gillies, S.J. Matthews, and L.H. Sutcliffe, Magn. Reson. Chem. **30**, 259 (1992).

[39] K.G. Conn, P.A. Beckmann, C.W. Mallory, and F.B. Mallory, J. Chem. Phys. **87**, 20 (1987).

[40] P.A. Beckmann, H.A. Al-Hallaq, A.M. Fry, A.L. Plofker, B.A. Roe, and J.A. Weiss, J. Chem. Phys. **100**, 752 (1994).